We are IntechOpen, the world's leading publisher of Open Access books Built by scientists, for scientists

4,800
Open access books available

122,000
International authors and editors

135M
Downloads

Our authors are among the

154
Countries delivered to

TOP 1%
most cited scientists

12.2%
Contributors from top 500 universities

CLARIVATE ANALYTICS BOOK CITATION INDEX INDEXED

WEB OF SCIENCE™

Selection of our books indexed in the Book Citation Index in Web of Science™ Core Collection (BKCI)

Interested in publishing with us?
Contact book.department@intechopen.com

Numbers displayed above are based on latest data collected.
For more information visit www.intechopen.com

Chapter 10

Identification of Key Molecules Involved in the Protection of Vultures Against Pathogens and Toxins

Lourdes Mateos-Hernández, Elena Crespo,
José de la Fuente and José M. Pérez de la Lastra

Additional information is available at the end of the chapter

http://dx.doi.org/10.5772/54191

1. Introduction

Vultures may have one of the strongest immune systems of all vertebrates (Apanius et al., 1983; Ohishi et al., 1979). Vultures are unique vertebrates able to efficiently utilize carcass from other animals as a food resource. These carrion birds are in permanent contact with numerous pathogens and toxins found in its food. In addition, vultures tend to feed in large groups, because carcasses are patchy in space and time, and feeding often incurs fighting and wounding, exposing vultures to the penetration of microorganisms present in the carrion (Houston & Cooper, 1975). When an animal dies, the carcass provides the growth conditions necessary for many pathogens to thrive and produce high levels of toxins. Vultures are able to feed upon such a carcasses with no apparent ill effects. Therefore, vultures were predicted to have evolved immune mechanisms to cope with a high risk of infection with virulent parasites.

Despite the potential interest in carrion bird immune system, little is known about the molecular mechanisms involved in the regulation of this process in vultures. The aim of this chapter was to explore the genes from the griffon vulture (*Gyps fulvus*) leukocytes, particularly to search novel receptors, such as the toll-like receptor (TLRs) and other components involved in the immune sensing of pathogens and in the mechanism by which vulture are protected against toxins. This study is, to the best of our knowledge, the first report of exploring the transcriptome in this interesting specie.

The toll-like receptor (TLR) family is an ancient pattern recognition receptor family, conserved from insects to mammals. Members of the TLR family are vital to immune function through the sensing of pathogenic agents and initiation of an appropriate immune

response. The rapid identification of Toll orthologues in invertebrates and mammals suggests that these genes must be present in other vertebrates (Takeda, 2005). During the recent years, members of the multigene family of TLRs have been recognised as key players in the recognition of microbes during host defence (Hopkinsn & Sriskandan, 2005). Recognition of pathogens by immune receptors leads to activation of macrophages, dendritic cells, and lymphocytes. Signals are then communicated to enhance expression of target molecules such as cytokines and adhesion molecules, depending on activation of various inducible transcription factors, among which the family NF-kappaB transcription factors plays a critical role. The involvement of nuclear factor-kappa B (NF-κB) in the expression of numerous cytokines and adhesion molecules has supported its role as an evolutionarily conserved coordinating element in organism's response to situations of infection, stress, and injury. In many species, pathogen recognition, whether mediated via the Toll-like receptors or via the antigen-specific T- and B-cell receptors, initiates the activation of distinct signal transduction pathways that activate NF-κB (Ghosh et al., 1998). TLR-mediated NF-κB activation is also an evolutionarily conserved event that occurs in phylogenetically distinct species ranging from insects to mammals.

Botulinun toxins are the most deadly neurotoxins known to man and animals. When an animal dies from botulism or other causes, the carcass provides the growth conditions necessary for *C. botulinun* to thrive and produce high levels of toxins. Certain species of carrion-eater birds and mammals are able to feed upon such carcasses with no apparent ill effects. Turkey vultures (*Cathartes aura*), have been shown to be highly resistant to botulinun toxins (Kalmbach, 1993; Pates, 1967, cited by Oishi et al., 1979). The mechanism by which these species are protected against botulinun toxin was investigated by exploring the genes from the griffon vulture (*Gyps fulvus*) leukocytes, particularly with the identification of ORFs with homology to the Ras-related botulinun toxin substrate 2 (RAC2), ADP-ribosylation factor 1 (a GTP-binding protein that functions as an allosteric activator of the cholera toxin catalytic subunit); a ras-related protein Rabb-11-B-like, and other ORFs with homology to some chemical mediators, such as IL-8, Chemokine (C-C motif) ligand 1.

2. Exploring the genes from the griffon vulture (*Gyps fulvus*) leukocytes

Given that the vulture is protected in Spain, we have used an *ex-vivo* approach. We have generated a cDNA library from from vulture peripheral blood monuclear cells (PBMC) and screened it, either with specific probes or randomly, to search for molecules involved in the immune recognition of pathogens and in the mechanism of resistance to toxins. In order to search for molecules involved in the immune recognition of pathogens and in the mechanism of resistance to toxins, we screened the cDNA library randomly. Several clones were identified and sequenced from the screening of the cDNA library from vulture´s leukocytes. A total of 49 open reading frames (ORFs) were identified by BLAST analysis from 100 plaques approximately. The identification and function of each ORF are summarized in the Table 1.

http://dx.doi.org/10.5772/54191

ORF /Acs number	Function	Assignment[1]
Phosphogycerato kinase 1 PGK1 JX889400	Glycolytic enzyme, also PGK-1 may acts as a polymerase alpha cofactor protein (primer recognition protein).	CA
Activity-dependent neuroprotector homeobox (ADNP) JX889402	Potential transcription factor. May mediate some of the neuroprotective peptide VIP-associated effects involving normal growth and cancer proliferation.	RP
Serpin B5-like JX889399	Tumor suppressor. It blocks the growth, invasion, and metastatic properties of mammary tumors.	RP
40S ribosomal protein S3a JX889382	May play a role during erythropoiesis through regulation of transcription factor DDIT3.	OT
Mps one binder kinase activator-like 1B, JX889412	Activator of LATS1/2 in the Hippo signaling pathway which plays a pivotal role in organ size control and tumor suppression by restricting proliferation and promoting apoptosis.	OT
Lymphocyte antigen 86 [LY86] JX889396	May cooperate with CD180 and TLR4 to mediate the innate immune response to bacterial lipopolysaccharide (LPS) and cytokine production. Important for efficient CD180 cell surface expression.	IS
IL-8 JX889394	Chemotactic factor that attracts neutrophils, basophils, and T-cells, but not monocytes. It is also involved in neutrophil activation. It is released from several cell types in response to an inflammatory stimulus.	IS
Constitutive coactivator of PPAR-gamma-like protein 1, JX889388	May participate in mRNA transport in the cytoplasm. Critical component of the oxidative stress-induced survival signaling.	OT
Interferon regulatory factor 1 (IRF-1), JX889416	Specifically binds to the upstream regulatory region of type I IFN and IFN-inducible MHC class I genes and activates those genes. Acts as a tumor suppressor.	IS
Annexin A1 [ANXA1], JX889410	Calcium/phospholipid-binding protein which promotes membrane fusion and is involved in exocytosis. This protein regulates phospholipase A2 activity.	RP
Chemokine (C-C motif) ligand 1, JX889398	Cytokine that is chemotactic for monocytes but not for neutrophils. Binds to CCR8	IS
Ras-related C3 botulinum toxin substrate 2 (RAC2) JX889392	Enzyme regulation: Plasma membrane-associated small GTPase which cycles between an active GTP-bound and inactive GDP-bound state. In active state binds to a variety of effector proteins to regulate cellular responses, such as secretory processes, phagocytose of apoptotic cells and epithelial cell polarization. Augments the production of reactive oxygen species (ROS) by NADPH oxidase	IS
Activating transcription factor 4 (ATF4), JX889393	Transcriptional activator. Binds the cAMP response element (CRE), a sequence present in many viral and cellular promoters.	RP
Elongation factor 1-alpha 1 (EF-1-alpha-1), JX889383	This protein promotes the GTP-dependent binding of aminoacyl-tRNA to the A-site of ribosomes during protein biosynthesis	OT
Polynucleotide 5'-hydroxyl-kinase NOL9, JX889408	Polynucleotide 5'-kinase involved in rRNA processing.	RP
Sodium/potassium -transporting ATPase subunit alpha-1, JX889386	Catalytic activity: Catalytic component of the active enzyme, which catalyzes the hydrolysis of ATP coupled with the exchange of sodium and potassium ions across the plasma membrane. This action creates the electrochemical gradient of sodium and potassium ions, providing the energy for active transport of various nutrients.	CA
Tyrosyl-DNA phosphodiesterase 2 (TDP2), JX889415	DNA repair enzyme that can remove a variety of covalent adducts from DNA through hydrolysis of a 5'-phosphodiester bond, giving rise to DNA with a free 5' phosphate.	OT
Transaldolase (EC 2.2.1.2) [TALDO1] JX889384	Important for the balance of metabolites in the pentose-phosphate pathway.	CA
60S ribosomal	Binds to a specific region on the 26S rRNA	RP

protein L23a variant 1, JX889411		
2',3'-cyclic-nucleotide 3'-phosphodiesterase (EC 3.1.4.37) (CNP), JX889397	Catalytic activity: Nucleoside 2',3'-cyclic phosphate + H(2)O = nucleoside 2'-phosphate	CA
Ribosomal protein S6 (RPS6), JX889418	May play an important role in controlling cell growth and proliferation through the selective translation of particular classes of mRNA.	RP
Hippocalcin-like protein 1 (Protein Rem-1), JX889389	May be involved in the calcium-dependent regulation of rhodopsin phosphorylation	OT
Sel-1 suppressor of lin-12-like	May play a role in Notch signaling. May be involved in the endoplasmic reticulum quality control (ERQC) system also called ER-associated degradation (ERAD) involved in ubiquitin-dependent degradation of misfolded endoplasmic reticulum proteins.	IS
Arf-GAP domain and FG repeats-containing protein 1-like, JX889409	Required for vesicle docking or fusion during acrosome biogenesis. May play a role in RNA trafficking or localization. In case of infection by HIV-1, acts as a cofactor for viral ISRev and promotes movement of Rev-responsive element-containing RNAs from the nuclear periphery to the cytoplasm.	OT
TNF receptor-associated factor 6 (TRAF-6) JX889385	E3 ubiquitin ligase that, together with UBE2N and UBE2V1, mediates the synthesis of 'Lys-63'-linked-polyubiquitin chains conjugated to proteins, such as IKBKG, AKT1 and AKT2. Seems to also play a role in dendritic cells (DCs) maturation and/or activation. Represses c-Myb-mediated transactivation, in B lymphocytes. Adapter protein that seems to play a role in signal transduction initiated via TNF receptor, IL-1 receptor and IL-17 receptor.	IS
Sorting nexin-5, JX889390	May be involved in several stages of intracellular trafficking.	OT
F-box protein 34 (FBXO34), JX889403	Substrate-recognition component of the SCF (SKP1-CUL1-F-box protein)-type E3 ubiquitin ligase complex	OT
Low density lipoprotein receptor-related protein 5 (LRP5) JX889414	Component of the Wnt-Fzd-LRP5-LRP6 complex that triggers beta-catenin signaling through inducing aggregation of receptor-ligand complexes into ribosome-sized signalsomes.	IS
Coronin, actin binding protein 1C JX889404	May be involved in cytokinesis, motility, and signal transduction.	CM
tumor protein, translationally-controlled 1 (TPT1) JX889417	Involved in calcium binding and microtubule stabilization.	CM
SH3 domain binding glutamic acid-rich protein like (SH3BGRL) JX889401	Acts as a transcriptional regulator of PAX6. Acts as a transcriptional activator of PF4 in complex with PBX1 or PBX2. Required for hematopoiesis, megakaryocyte lineage development and vascular patterning.	RP
GATA-binding factor 2 (GATA-2) (Transcription factor NF-E1b) JX889387	Transcriptional activator, which regulates endothelin-1 gene expression in endothelial cells. Binds to the consensus sequence 5'-AGATAG-3'	RP
Cytochrome b5 JX889381	Membrane bound hemoprotein which function as an electron carrier for several membrane bound oxygenases, including fatty acid desaturases	OT
iron sulfur cluster assembly 1 homolog mitochondria JX889395	Acts as a co-chaperone in iron-sulfur cluster assembly in mitochondria	OT

Table 1. ORFs found from the random screening of the vulture leukocyte cDNA library. Assignment of the function of each ORF was performed based on the information shown at the Universal Protein Resource (UniProt) web page (http://www.uniprot.org/) and it was assigned as immune system (IS), Catalytic activity (CA), Cell motility (CM), Regulatory protein (RP) and Other (OT).

Interestingly, we found ORFs with homology to the Ras-related botulinun toxin substrate 2 (RAC2); the interferon regulatory factor I (IRF1), ADP-ribosylation factor 1 (a GTP-binding

http://dx.doi.org/10.5772/54191

protein that functions as an allosteric activator of the cholera toxin catalytic subunit); a ras-related protein Rabb-11-B-like; some chemical mediators, such as IL-8, Chemokine (C-C motif) ligand 1, etc. These sequences were deposited in the Genbank under accession numbers indicated in Table 1.

The *ras* and *ras-related* genes represent a superfamily coding for low molecular weight GTPases (Bourne et al., 1991). These proteins, which share significant homology in the four regions shown for the H-ras protein to be involved in the binding and hydrolysis of GTP, regulate a diverse number of cellular processes including growth and differentiation, vesicular trafficking, and cytoskeleton organization. GTPases are in an active state when GTP is bound and are inactive when GDP is bound, and a variety of additional proteins have been identified that regulate the switch between active and inactive states. ADP-ribosylation of cellular proteins by a number of bacterial toxins (*i.e.* cholera, pertussis, pseudomonas exotoxins A., and diphtheria) is the primary mechanism for their toxicity (Eidels et al., 1983). Botulinun toxins C1 and D contain an ADP-ribosyltransferase activity that is able to ADP-ribosylate 21-26 kDa eukaryotic proteins. The ORF found with high homology to the Ras-related botulinun toxin substrate 2 (RAC2) led us to hypothesize that this ORF is candidate for such a regulatory function in the vulture and it may be involved in the protection of vultures against toxins.

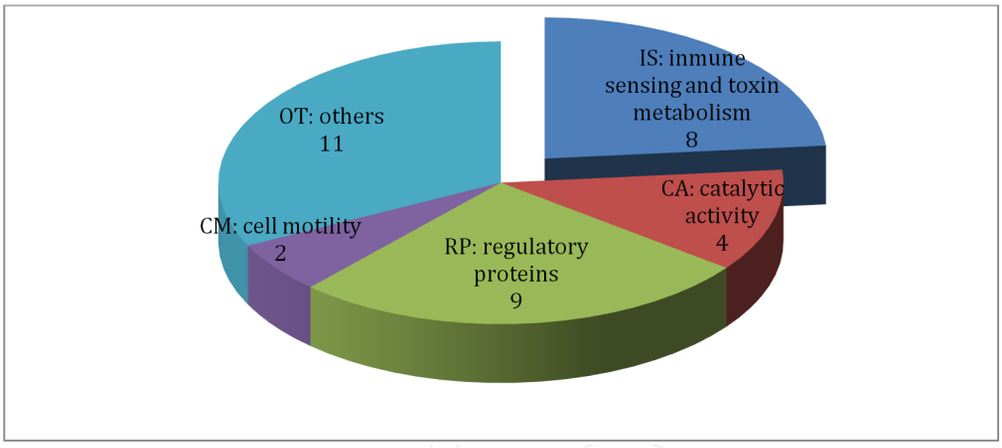

Figure 1. Pie-chart showing number of ORFs with different functions.

3. Strategy for cloning of vulture TLR1 and IκBα

In order to identify key components of the vulture system for sensing of pathogens, we screened a cDNA library from vulture peripheral blood monuclear cells (PBMC) using specific probes for TLR1 and IκBα.

Since the majority of toll-like receptors are expressed in leukocytes and lymphoid tissues in human and other vertebrates, we decided to use vulture PBMC as the source of RNA to obtain a specific probes for TLR1 and IκBα and to construct a cDNA library. Using this strategy we cloned cDNAs encoding for griffon vulture (*Gyps fulvus*) orthologues of mammalian

TLR1 (CD281) and for the alpha inhibitor of NF-κB (IκBα). The tissue and cell expression pattern of vulture TLR1 and IκBα were analyzed by real-time RT-PCR and correlated with the ability to respond to various pathogenic challenges.

3.1. Design of specific probes for vulture TLR1 and IκBα

To obtain specific probes for vulture TLR1 and IκBα, total RNA was isolated from vulture PBMC and from cells and tissues using the Ultraspec isolation reagent (Biotecx Laboratories, Houston TX, USA). Ten micrograms of total RNA was heated at 65 °C for 5 min, quenched on ice for 5 min and subjected to first strand cDNA synthesis. The RNA was reverse transcribed using an oligo dT12 primer by incubation with 200 U RNase H- reverse transcriptase (Invitrogen, Barcelona, Spain) at 25°C for 10 min, then at 42°C for 90 min in the presence of 50 mM Tris-HCl, 75 mM KCl, 3 mM MgCl2, 10 mM DTT, 30 U RNase-inhibitor and 1mM dNTPs, in a total volume of 20 μl.

For the vulture TLR probe, a partial fragment of 567 bp showing sequence similarity to human TLR-1 was amplified by PCR from vulture PBMC cDNA using two oligonucleotide primers TLR1/2Fw (5'-GAT TTC TTC CAG AGC TG–3') and TLR1/3Rv (5'-CAA AGA TGG ACT TGT AAC TCT TCT CAA TG -3'), which were designed based on regions of high homology among the sequences of human and mouse TLR1 (GenBank, accession numbers NM_003263 and NM_030682, respectively). Cycling conditions were 94°C for 30 s, 52°C for 30 s and 72°C for 1.5 min, for 30 cycles.

For the vulture IκBα probe, a partial fragment of 336 bp showing sequence similarity to human and chicken IκBα was amplified by PCR from vulture PBMC cDNA using two oligonucleotide primers IκBα-Fw (5'-CCT GAA CTT CCA GAA CAA C-3') and IκBα-Rv (5'-GAT GTA AAT GCT CAG GAG CCA TG-3'), which were designed based on regions of high homology among the sequences of human and chicken IκBα (GenBank, accession numbers M69043 and S55765, respectively). Cycling conditions were 94°C for 30 s, 52°C for 30 s and 72°C for 1.5 min, for 30 cycles.

The obtained PCR products were cloned into pGEM-T easy vector using a TA cloning kit (Promega, Barcelona, Spain) and sequenced bidirectionally to confirm their respective specificities. These fragments were DIG-labelled following the recommendation of the manufacturer (Roche, Barcelona, Spain) and used as probes to screen 500 000 plaque colonies of the vulture-PBMC cDNA library.

3.2. cDNA library construction and screening

Total RNA (500 μg) was extracted from PBMC (pooled from 6 birds) using the Ultraspec isolation reagent (Biotecx). mRNA (20 μg) was extracted by Dynabeads (Dynal biotech-Invitrogen, Barcelona, Spain) and used in the construction of a cDNA library in Lambda ZAP vector (Stratagene, La Jolla, CA, USA) by directional cloning into EcoRI and XhoI sites. The cDNA library was plated by standard protocols at 50 000 plaque forming units (pfu) per plate and grown on a lawn of XL1-Blue E. coli for 6-8 h. Screening of the library was performed with DIG labelled probes. Plaques were transferred onto Hybond-N+ membranes

(Amersham, Barcelona, Spain) denatured in 1.5 M NaCl/0.5M NaOH, neutralised in 1.5 M NaCl/0.5 Tris (pH 8.0) and fixed using a cross-linker oven (Stratagene). The filters were then pre-incubated with hybridisation buffer (5XSSC [1XSSC is 150 mM NaCl, 15 mM trisodium citrate, pH 7.7], 0.1% N-laurylsarcosine, 0.02% SDS and 1% blocking reagent (Roche)) at 65 °C for 1 h and then hybridised with hybridisation buffer containing the DIG-labelled probe, overnight at 65 °C. The membranes were washed at high stringency (2XSSC, 0.1% SDS; 2x5 min at ambient temperature followed by 0.5XSSC, 0.1% SDS; 2x15 min at 65 °C). DiG-labelled probes were detected using phosphatase-labelled anti-digoxygenin antibodies (Roche) according to the manufacturer's instructions. Positive plaques on membranes were identified, isolated in agar plugs, eluted in 1 ml of SM buffer (0.1M NaCl, 10 mM MgSO4, 0.01% gelatin, 50 mM Tris-Hcl, pH 7.5) for 24 h at 4°C and replated. The above screening protocol was then repeated. Individual positive plaques from the secondary screening were isolated in agar plugs and eluted in SM buffer. The cDNA inserts were recovered using the Exassist/SOLR system (Stratagene). Individual bacterial colonies containing phagemid were grown up in LB broth (1% NaCl, 1% trytone, 0.5% yeast extract, pH 7.0) containing 50 μg/ml ampicillin. Phagemid DNA was purified using a Bio-Rad plasmid mini-prep kit and sequenced.

4. Structural analysis of vulture TLR1 and IκB*α* sequences

Sequences were analyzed using the analysis software LaserGene (DNAstar, London, UK) and the analysis tools provided at the expasy web site (http://www.expasy.org). PEST regions are sequences rich in Pro, Glu, Asp, Ser and Thr, which have been proposed to constitute protein instability determinants. The analysis of the PEST region for the putative protein was made using the webtool PESTfind at http://www.at.embnet.org/toolbox/pestfind. The potential phosphorylation sites were calculated using the NetPhos 2.0 prediction server at http://www.cbs.dtu.dk/services/NetPhos. The prediction of the potential attachment of small ubiquitin-related modifier (SUMO) was made using the webtool SUMOplot™.

The alignment of vulture TIR domain sequences with TLR-1 from other species and of the vulture IκB*α* sequences with IκB*α* from other species was done using the program ClustalW v1.83 with Blosum62 as the scoring matrix and gap opening penalty of 1.53. Griffon vulture TLR-1 and IκB*α* sequences were deposited in the Genbank under accession numbers DQ480086 and EU161944, respectively.

4.1. Vulture TLR1

The screening of the vulture PBMC cDNA library for TLR1 yielded seven clones with identical open reading frame (ORF) sequences. The fact that the screening of 500,000 vulture cDNA clones resulted in 7 identical sequences suggested that this TLR receptor is broadly represented in PBMC, possibly illustrating its important role in pathogen recognition during vulture innate immune response. This result was consistent with the real time RT-PCR analysis of TLR1 transcripts in vulture cells.

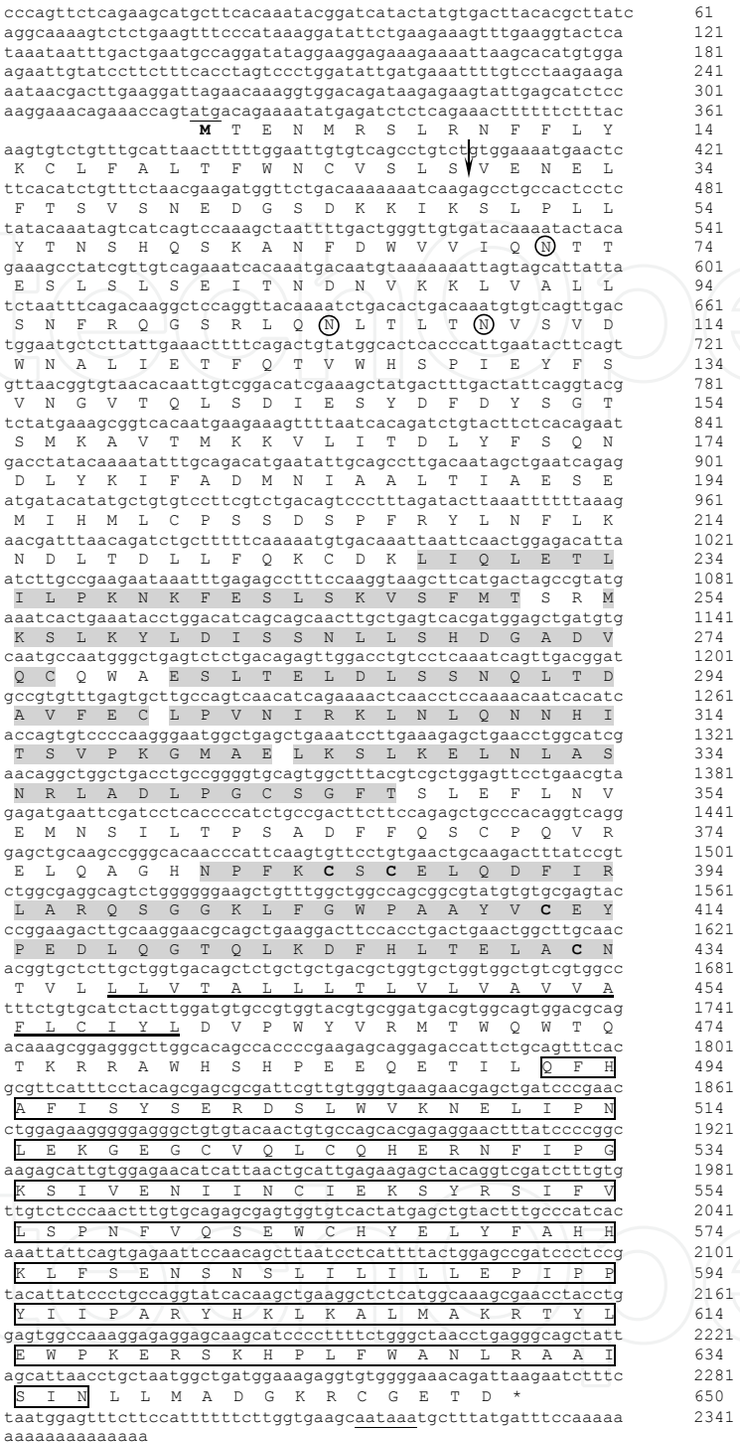

Figure 2. Nucleotide and deduced amino acid sequence of vulture TLR1. Complete sequence of the full-length Vulture TLR obtained from the cDNA library (GenBank accession number: DQ480086). Translated amino acid sequence is also shown under nucleotide sequence. Numbers to the right of each row refer to nucleotide or amino acid position. The cleavage site for the putative signal peptide is indicated by an arrow. LRRs domains are shaded. Potential N-glycosylation sites are circled. The predicted transmembrane segment is underlined. The initiation codon (atg) and the polyadenilation site are underlined. The translational stop site is indicated by an asterisk. The cysteines critical for the maintenance of the structure of LRR-CT are in bold.

http://dx.doi.org/10.5772/54191

The largest clone (2,355 bp) contained an ORF that encoded a 650 amino acid putative vulture orthologue to TLR1, flanked by 319 bp 5'UTR and a 83 bp 3'UTR that contained a potential polyadenylation signal, AATAAA, 21 bp upstream of the poly (A) tail (Fig. 2). The predicted molecular weight of the putative vulture TLR1 was of 74.6 KDa. The predicted protein sequence had a signal peptide, an extracellular portion, a short transmembrane region and a cytoplasmic segment (Fig. 2). In assigning names to the vulture TLR, we looked at the closest orthologue in chicken and followed the nomenclature that was proposed for this species (Yilmaz et al., 2005). Therefore, the discovered sequence was identified as vulture TLR1.

4.1.1. Amino acid sequence comparison of vulture TLR1 with other species

The comparison of the deduced amino acid sequence of vulture TLR1 with the sequence of chicken, pig, cattle, human and mouse TLR1 indicated that the deduced protein had a higher degree of similarity to chicken (64% of amino acid similarity) than to pig (51%), cattle (51%), human (51%) and mouse (48%) sequences (Fig. 3). Protein sequence similarity was different on different TLR domains (Fig. 3).

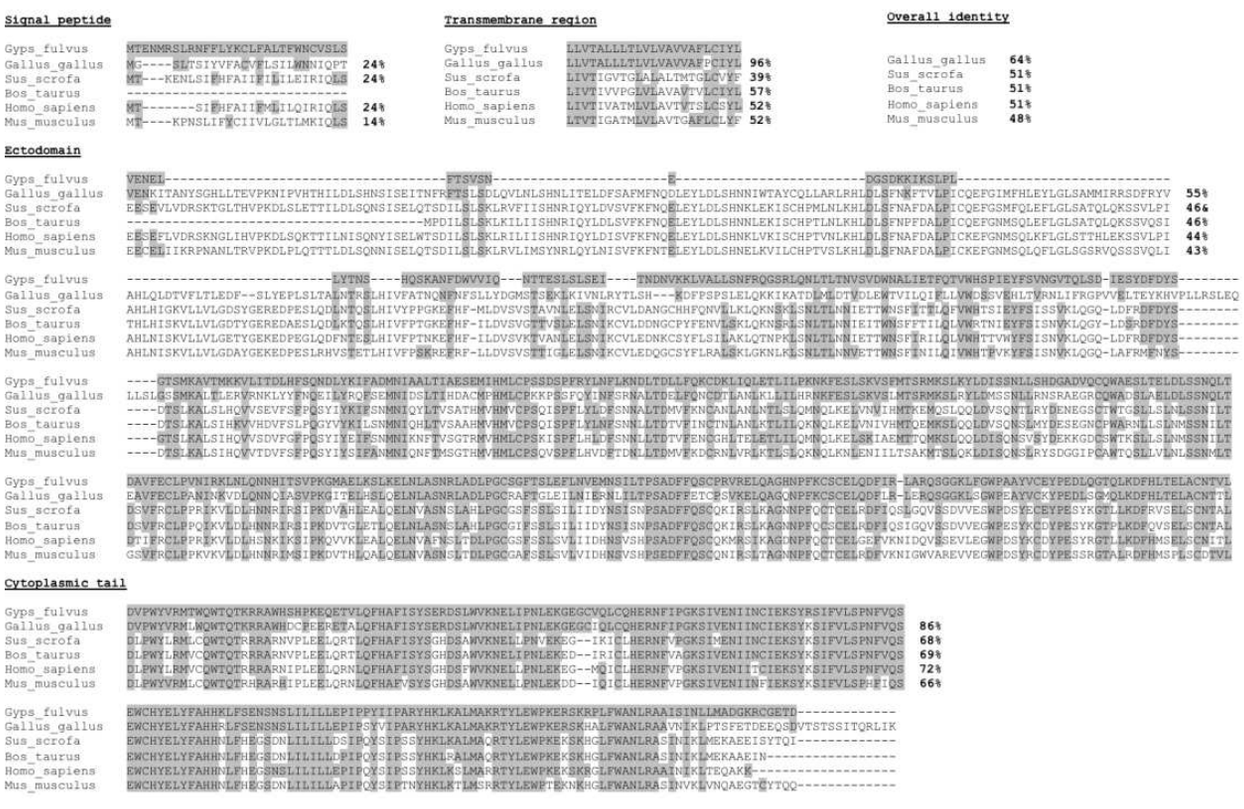

Figure 3. Alignment of amino acid sequences of TLR1 from different species.

Amino acid sequence of vulture TLR1 was aligned with the orthologous sequence of chicken (*Gallus gallus*), pig (*Sus scrofa*), cattle (*Bos taurus*), human (*Homo sapiens*) and mouse (*Mus musculus*) based on amino acid identity and structural similarity. Identical amino acid resi-

dues to vulture TLR1 from the aligned sequences are shaded. Gaps were introduced for optimal alignment of the sequences and are indicated by dashes (-). GenBank or Swiss protein accession numbers are: DQ480086, Q5WA51, Q59HI9, Q706D2, Q5FWG5 and Q6A0E8, respectively.

For the TLRs, it is assumed that the structure of the ectodomain has evolved more quickly than the structure of the TIR (Johnson et al., 2003). Similarly to other TLR receptors, the degree of homology of vulture TLR1 was higher in the transmembrane and cytoplasmic domains than in the extracellular domain.

The vulture TLR1 with 650 amino acids is probably the TLR with the shortest length and the smallest predicted MW (74.6 kDa). Recently, a chicken isoform of TLR1 (Ch-TLR1 type 2) was identified *in silico* and predicted to have a similar number of residues than vulture TLR1 (Yilmaz et al., 2005). However, this receptor also contains an additional transmembrane region in its N-terminal end, and the pattern of expression in tissues is also different from that ChTLR1 type 1 (Yilmaz et al., 2005).

Comparison of the structure obtained from the SMART analysis (at expasy web server) of the amino acid sequence from human, bovine, pig, mouse, chicken and vulture TLR1. Each diagram shows a typical structure of a member of the toll-like receptor family. Vulture TLR1 consists of an ectodomain containing five leucine rich repeats (LRRs) followed by an additional leucine rich repeat C terminal (LRR-CT) motif. The Vulture TLR has a transmembrane segment and a cytoplasmic tail which contains the TIR domain. Genbank or swiss accession number for proteins are DQ480086 (vulture), Q5WA51 (chicken), Q59HI9 (pig), Q706D2 (bovine), Q5FWG5 (human) and Q6A0E8 (mouse).

Structural feature	*G fulvus*	*G gallus*	*S scrofa*	*B taurus*	*H sapiens*	*M musculus*
Amino acid residues	650	818	796	727	786	795
Number of LRRs	5	5	5	5	4	6
N-glycosylation sites	3	5	4	6	7	8
Predicted MW(KDa)	74.60	94.46	90.94	83.04	90.29	90.67
Length of ectodomain	409	569	560	521	560	558

Table 2. Structural features of TLR1 receptor from Griffon vulture (*G. fulvus*), Chicken (*G. gallus*), pig (*S. scrofa*), cattle (*B. taurus*) human (*H. sapiens*) and mouse (*M. musculus*) amino acid sequences. The theoretical molecular weight, number of LRRs, and of glycosilation sites was calculated using the software available at the expasy web server (http://www.expasy.org). Genbank or Swiss accession number for proteins are DQ480086 (*G. fulvus*), Q5WA51 (*G. gallus*), Q59HI9 (*S. scrofa*), Q706D2 (*B. taurus*), Q5FWG5 (*H. sapiens*) and Q6A0E8 (*M. musculus*).

http://dx.doi.org/10.5772/54191

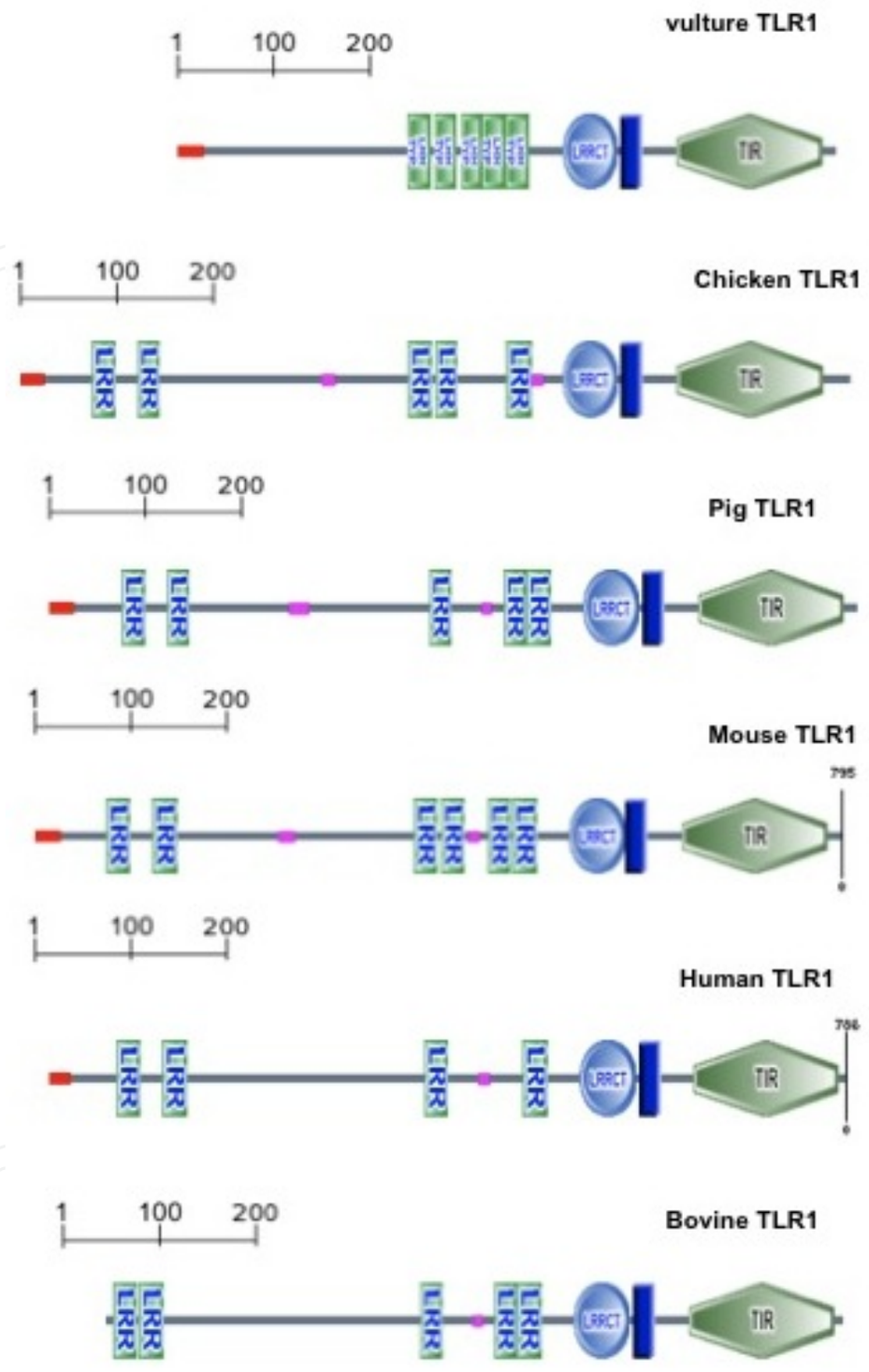

Figure 4. Schematic structure of TLR1 from various species

In general, the structure of vulture TLR1 shows similarity to chicken and mammalian TLR1 (Table 2). However, vulture TLR1 exhibits some structural features that could influence its functional role as pathogen receptor (Fig. 4). For example, it is possible that the smaller size

of vulture TLR1, the lower number of N-glycosylation sites and the grouping of its LRRs in the proximal half of its ectodomain have functional implications.

The set of Toll proteins for humans and insects each contain widely divergent LRR regions, and this is viewed as providing the potential to discriminate between different ligands. Perhaps these features provide vulture TLR1 some advantages on pathogen recognition. TLR glycosylation is also likely to influence receptor surface representation, trafficking and pattern recognition (Weber et al., 2004).

4.2. Vulture IκBα

The screening of the vulture PBMC cDNA library yielded one clone that contained an ORF that encoded a 313 amino acid putative vulture orthologue to IκBα, flanked by 15 bp 5'UTR and a 596 bp 3'UTR (Fig. 5).

```
cggagccctgccgctatgatcagcgcccgccgcctcgtcgagccgccggttatggagggc   60
 M  I  S  A  R  R  L  V  E  P  P  V  M  E  G    15
tacgagcaagcgaagaaagagcgccagggcggcttcccgctcgacgaccgccacgacagc   120
 Y  E  Q  A  K  K  E  R  Q  G  G  F  P  L  D  D  R  H  D  S    35
ggcttggactccatgaaggaggaagagtaccggcagctggtgaaggagctggaggacata   180
 G  L  D  S  M  K  E  E  E  Y  R  Q  L  V  K  E  L  E  D  I   55
cgcctgcagccccgcgagccgcccgcctgggcgcagcagctgacggaggacggagacact   240
 R  L  Q  P  R  E  P  P  A  W  A  Q  Q  L  T  E  D  G  D  T    75
tttctccacttggcgattattcacgaggaaaaagccctgagcctggaggtgatccggcag   300
 F  L  H  L  A  I  I  H  E  E  K  A  L  S  L  E  V  I  R  Q    95
gcggccggggaccgtgctttcctgaacttccagaacaacctcagccagactcctcttcac   360
 A  A  G  D  R  A  F  L  N  F  Q  N  N  L  S  Q  T  P  L  H   115
ctggcagtgatcaccgatcagcctgaaattgccgagcatcttctgaaggccggatgcgac   420
 L  A  V  I  T  D  Q  P  E  I  A  E  H  L  L  K  A  G  C  D   135
ctggaactcagggacttccgaggaaacacccccctgcatattgcctgccagcagggctcc   480
 L  E  L  R  D  F  R  G  N  T  P  L  H  I  A  C  Q  Q  G  S   155
ctcaggagcgtcagcgtcctcacgcagtactgccagccgcaccacctcctcgctgtcctg   540
 L  R  S  V  S  V  L  T  Q  Y  C  Q  P  H  H  L  L  A  V  L   175
caggcaaccaactacaacgggcatacatgtctccatttggcatctattcaaggatacctg   600
 Q  A  T  N  Y  N  G  H  T  C  L  H  L  A  S  I  Q  G  Y  L   195
cctattgtcgaatacttgctgtccttgggagcagatgtaaatgctcaggagccatgcaat   660
 A  I  V  E  Y  L  L  S  L  G  A  D  V  N  A  Q  E  P  C  N   215
ggcagaacggcactacatttggctgtcgacctgcagaattcagacctggtgtcgcttctg   720
 G  R  T  A  L  H  L  A  V  D  L  Q  N  S  D  L  V  S  L  L   235
gtgaaacatggggcggacgtgaacaaagtgacctaccaaggctattccccctatcagctc   780
 V  K  H  G  A  D  V  N  K  V  T  Y  Q  G  Y  S  P  Y  Q  L   255
acatggggaagagacaactccagcatacaggaacagctgaagcagctgaccacagccgac   840
 T  W  G  R  D  N  S  S  I  Q  E  Q  L  K  Q  L  T  T  A  D   275
ctgcagatgttgccagaaagtgaggacgaggagagcagtgaatcggagcctgaattcaca   900
 L  Q  M  L  P  E  S  E  D  E  E  S  S  E  S  E  P  E  F  T   295
gaggatgaacttatatacgatgactgccttattggaggacgacagctggcattttaaagc   960
 E  D  E  L  I  Y  D  D  C  L  I  G  G  R  Q  L  A  F  *      313
agagctatctgtgaaaagaagtgactgtgtacatatgtatagaaaaaggactgacttcat   1020
ttaaaaagaaagtcgcaatgcaaagggaaaaaccaggagggaaatactacactgcccagc   1080
aaggagcacataattgtaacaggttctggcctgtgtttaaatacaggagtgggatgtgta   1140
acatcagtagggatctgtgattattcacaccacctgataaagagccacatagccaatctt   1200
ctcagccctacaaaggtaacagactacacatccaacctgctggttacagagagctatctt   1260
gtggtgttaagtaccacgaggaatgcgtgtcgcctcgtggcaaggcaggctcataccaac   1320
ccccccatcttctcggagactgcgtgttaatctgcgttgggctggtggtgctccctggcc   1380
ttactgaccggcctcagctgctcttggtggggtgtcccaggtggaggagtcaaaccaagg   1440
gactggtgacctcctgactgttagaagaaagtagcaataatgttaactgtgggcattgga   1500
aactgtgtgtttcacaccatgtgtgtcataattgctacacttttagcaattg           1553
```

Figure 5. Nucleotide and deduced amino acid sequence of vulture IκBα. Complete sequence of the full-length vulture IκBα obtained from the cDNA library (GenBank accession number: EU161944). Translated amino acid sequence is also shown under nucleotide sequence. Numbers to the right of each row refer to nucleotide or amino acid position. Ankyrin domains are shaded. The PEST region is underlined. The ATTTA domain is in bold. Phosphorylation sites Ser-35 and Ser-39 are circled. The translational stop site is indicated by an asterisk.

http://dx.doi.org/10.5772/54191

The predicted molecular weight of the putative vulture IκBα was of 35170 Da. Structurally, the vulture I kappa B alpha molecule could be divided into three sections: a 70-amino-acid N terminus with no known function, a 205-residue midsection composed of five ankyrin-like repeats, and a very acidic 42-amino-acid C terminus that resembles a PEST sequence. Examination of the Griffon vulture sequence revealed the features characteristic of an IκB molecule (Fig. 6) The putative vulture IκBα protein was composed of a N-terminal regulatory domain, a central ankyrin repeat domain (ARD), required for its interaction with NF-κB, and a putative PEST-like sequence in the C-terminus (Fig. 6), which is similar to IκBα proteins from other organisms (Jaffray et al., 1995). Together with the N-terminal regulatory domain and the central ARD domain, the presence of an acidic C-terminal PEST region rich in the amino acids proline (P), glutamic acid (E), serine (S) and threonine (T) is characteristic of IκBα inhibitors (Luque & Gelinas, 1998). PEST regions have been found in the C-terminus of avian IκBα (Krishnan et al., 1995) and mammalian IκBα and it was also present in the vulture IκBα sequence (Fig. 6). Particularly, the PEST sequence of IκBα seems to be critical for its calpain-dependent degradation (Shumway et al., 1999).

Figure 6. Schematic structure of vulture IκBα.

Structure obtained from the SMART analysis (at expasy web server) of the amino acid sequence from vulture IκBα. Each box shows a typical structure of a member of the IκBα inhibitor. Vulture IκBα consists of an N-terminus regulatory domain, a central ankyrin domain containing five ankyrin repeats followed by an additional PEST-like motif. Number shows the amino acid flanking the relevant domains.

Classical activation of NF-kappaB involves phosphorylation, polyubiquitination and subsequent degradation of IκB (Figure. Several residues are known to be important in the N-terminal regulatory domain (Luque & Gelinas, 1998, Luque et al., 2000). In nonstimulated cells, NF-kappa B dimers are maintained in the cytoplasm through interaction with inhibitory proteins, the IκBs (Fig. 7).

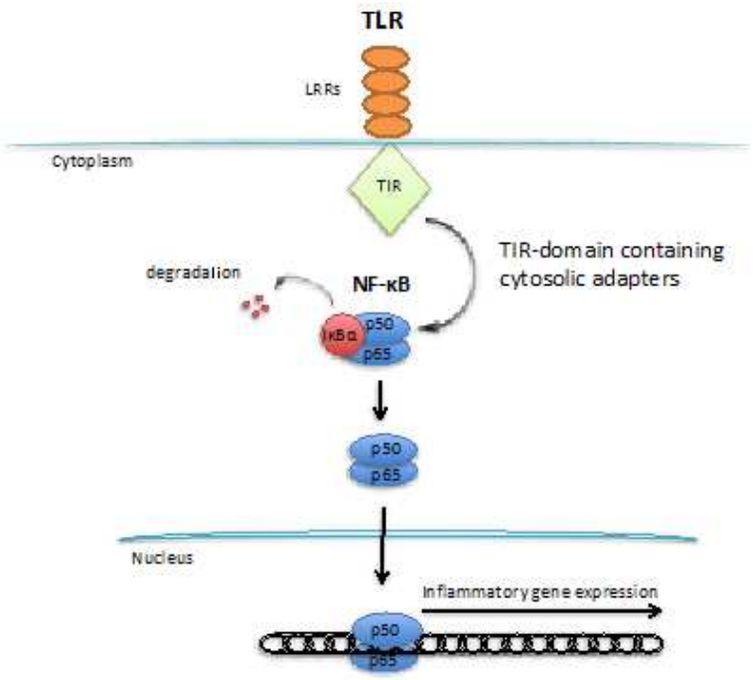

Figure 7. Activation of the NFκB pathway by TLRs. Ligand binding of TLR results in direct or indirect recruitment of a series of TIR-domain containing adapters, which in turn phosphorylates IκBs, causing degradation of the inhibitor and translocation of the transcription factor to the nucleus, where it initiates the transcription of genes encoding chemokines and pro-inflammatory cytokines.

In response to cell stimulation, mainly by proinflammatory cytokines, a multisubunit protein kinase, the I kappa B kinase (IKK), is rapidly activated and phosphorylates two critical serines in the N-terminal regulatory domain of the I kappa Bs. Phosphorylated IκBs are recognized by a specific E3 ubiquitin ligase complex on neighboring lysine residues, which targets them for rapid degradation by the 26S proteasome, which frees NFκ-B and leads to its translocation to the nucleus, where it regulates gene transcription (Karin & Ben-Neriah, 2000). It has been demonstrated that phosphorylation of the N-terminus residues Ser-32 and Ser-36 is the signal that leads to inducer-mediated degradation of IκB*α* in mammals (Brown et al., 1997; Good et al., 1996).

As can be observed in the alignment of Figure 8, the griffon vulture equivalent residues seem to be Ser-35 and Ser-39, which are part of the conserved sequence DSGLDS (Luque et al., 2000; Pons et al., 2007). This observation suggests that the phosphorylation of these serine residues could trigger the IκB*α* inducer-mediated degradation in vulture in a similar manner to that in mammals. Unlike ubiquitin modification, which requires phosphorylation of S32 and S36, the small ubiquitin-like modifier (SUMO) modification of IκB*α* is inhibited by phosphorylation. Thus, while ubiquitination targets proteins for rapid degradation, SUMO modification acts antagonistically to generate proteins resistant to degradation (Desterro et al., 1998; Mabb & Miyamoto, 2007). This SUMO modification occurs primarily on K21 (Mabb & Miyamoto, 2007). This residue was also conserved in the IκB*α* sequence from human, mouse, pig, rat and vulture, but not from chicken (Fig. 8).

http://dx.doi.org/10.5772/54191

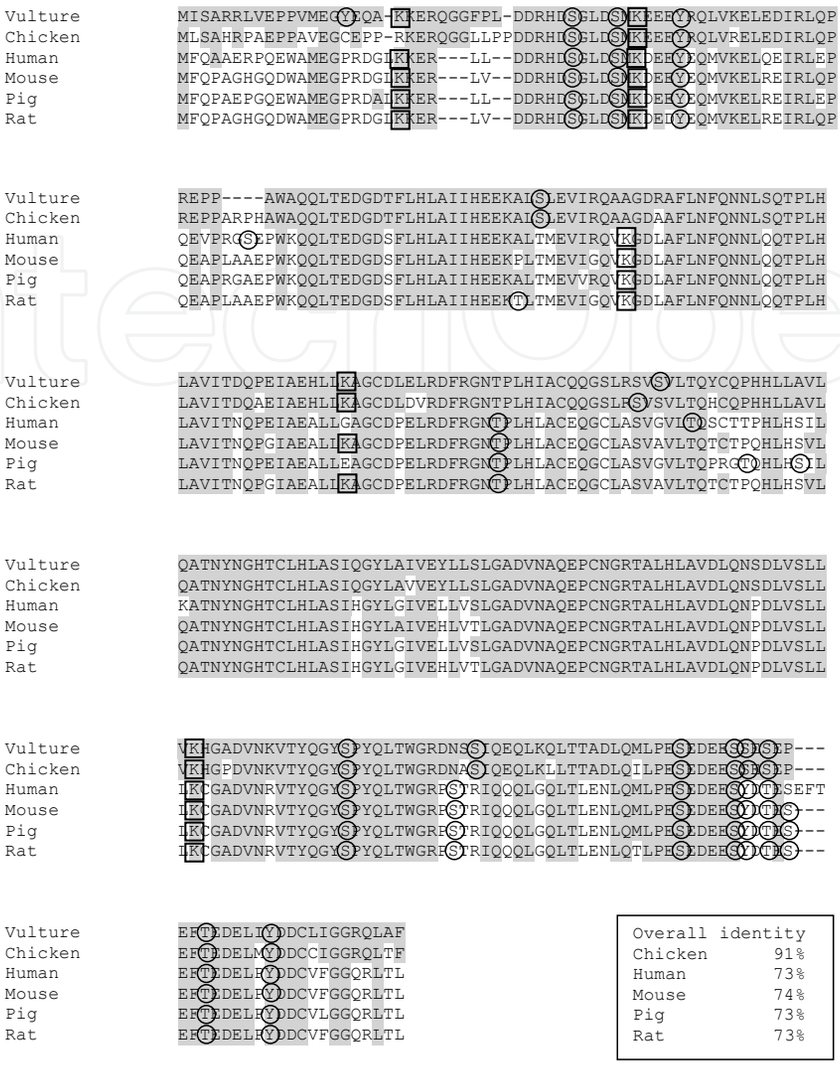

Figure 8. Alignment of amino acid sequences of IκBα from different species.

Amino acid sequence of vulture IκB*α* was aligned with the orthologous sequence of chicken (*Gallus gallus*), pig (*Sus scrofa*), cattle (*Bos taurus*), human (*Homo sapiens*) and mouse (*Mus musculus*) based on amino acid identity and structural similarity. Identical amino acid residues to vulture IκB*α* from the aligned sequences are shaded. Gaps were introduced for optimal alignment of the sequences and are indicated by dashes (-). SUMOlation sites are squared and phosphorylation sites are circled. GenBank or Swiss protein accession numbers are: DQ480086, Q5WA51, Q59HI9, Q706D2, Q5FWG5 and Q6A0E8, respectively. Griffon vulture IκB*α* sequence was deposited in the Genbank under accession number EU161944.

A common characteristic of the IκB proteins is the presence of ankyrin repeats, which interact with the Rel-homology domain of NF-κB (Aoki et al., 1996; Luque & Gelinas, 1998). In the vulture sequence, five ankyrin repeats were detected using the Simple Modular Architecture Research Tool (SMART) at EMBL (Table 2). Five ankyrin repeats also exist in human and other vertebrates IκB*α* (Jaffray et al., 1995). It is possible that individual repeats have

remained conserved because of their important structural and functional roles in regulating NF-κB.

Compared with other species, vulture IκBα exhibited the lowest number of predicted SUMOlation sites (Table 3).

Structural feature	*G fulvus*	*G gallus*	*H sapiens*	*S scrofa*	*R norvegicus*	*M musculus*
Amino acid residues	313	318	317	314	314	314
Number of ankyrin repeats	5	5	5	5	5	5
Phosphorylation sites	14	13	14	15	14	13
Predicted MW(KDa)	35,17	35,40	35,61	35,23	35,02	35,02
SUMOlation sites	2	3	4	4	5	5

Table 3. Structural features of IκBα from Griffon vulture (*G. fulvus*), Chicken (*G. gallus*), human (*H. sapiens*), pig (*S. scrofa*), rat (*R. norvegicus*) and mouse (*M. musculus*) amino acid sequences. The theoretical molecular weight, number of ankyrin repeats, SUMOlation and of phosphorylation sites was calculated using the software available at the expasy web server (http://www.expasy.org). Genbank or Swiss accession number for proteins are EU161944 (*G. fulvus*), Q91974 (*G. gallus*), P25963 (*H. sapiens*), Q08353 (*S. scrofa*), Q63746 (*R. norvegicus*), and Q9Z1E3 (*M. musculus*).

4.2.1. Amino acid sequence comparison of vulture IκBα with other species

The comparison of the deduced amino acid sequence of vulture IκBα with the sequence of chicken, human, mouse, pig, and rat IκBα indicated that the deduced protein had a higher degree of similarity to chicken (91% of amino acid similarity) than to human (73%), mouse (74%), pig (73%) and rat (73%) sequences (Fig. 7). The analysis of the vulture IκBα sequence using the software NetPhos 2.0 (cita) revealed 14 potential phosphorylation sites: 10 Ser (S35, S39, S89, S160, S251, S263, S282, S287, S288, and S290), 1 Thr (T295) and 3 Tyr (Y16, Y45, and Y301). Although many of these residues were conserved in the aligned sequences from chicken, human, mouse, pig and rat IκBα, two phosphorylation sites (Y16 and S160) were distinctive to the vulture sequence (Fig.8).

5. Detection of vulture TLR1 and IκBα expression in tissues

In order to better understand the biological roles of TLR1 and IκBα, we analyzed their tissue expression pattern. The presence of transcripts encoding vulture TLR1 and IκBα in tissues was determined by real time RT-PCR. Biological samples were collected from vultures (about 8-10 months old) that were provisionally captive at the Centre for Wild Life Protection, "El Chaparrillo", Ciudad Real, Spain. Blood was obtained by puncture of the branquial vein, located in the internal face of the wing, and collected in 10 ml tubes with EDTA as anticoagulant. Blood (10 ml) was diluted 1:1 (vol:vol) with PBS (Sigma) and the mononuclear fraction containing PBMC was obtained by density gradient centrifugation on Lymphoprep (Axis-Shield, Oslo, Norway). All vulture tissues used for cDNA preparation were obtained fresh from euthanised birds that were impossible to recover.

http://dx.doi.org/10.5772/54191

RT-PCR was performed on a SmartCycler® II thermal cycler (Cepheid, Sunnyvale, CA, USA) using the QuantiTect® SYBR® Green RT-PCR Kit (Quiagen, Valencia, CA, USA), following the recommendations of the manufacturer. We used primers GfTLR-Fw (5′-GCT TGC CAG TCA ACA TCA GA-3′) and GfTLR-Rv (5′-GAA CTC CAG CGA CGT AAA GC-3′), which amplify a fragment of 158 bp of vulture TLR1 and primers IκB*α* -L (5′- CTG CAG GCA ACC AAC TAC AA -3′) and IκB*α* –R (5′- TGA ATT CTG CAG GTC GAC AG-3′), which amplify a fragment of 165 b of vulture IκB*α*. Cycling conditions were: 94°C for 30 sec, 60°C for 30 sec, 72°C for 1 min, for 40 cycles. As an internal control, RT-PCR was performed on the same RNAs using the primers BA-Fw (5′-CTA TCC AGG CTG TGC TGT CC-3′) and BA-Rv (5′-TGA GGT AGT CTG TCA GGT CAG G-3′), which amplify a fragment of 165 bp from the conserved housekeeping gene beta-actin. Control reactions were done using the same procedures, but without RT to control for DNA contamination in the RNA preparations, and without RNA added to control contamination of the PCR reaction. Amplification efficiencies were validated and normalized against vulture beta actin, (GenBank accession number DQ507221) using the comparative Ct method. Experiments were repeated for at least three times with similar results. Tissues used for the study were artery, liver, lung, bursa cloacalis, heart, small intestine, peripheral blood mononuclear cells (PBMC), large intestine and kidney.

The level of TLR1 mRNA was higher in kidney, small intestine and PBMC (Fig. 9).

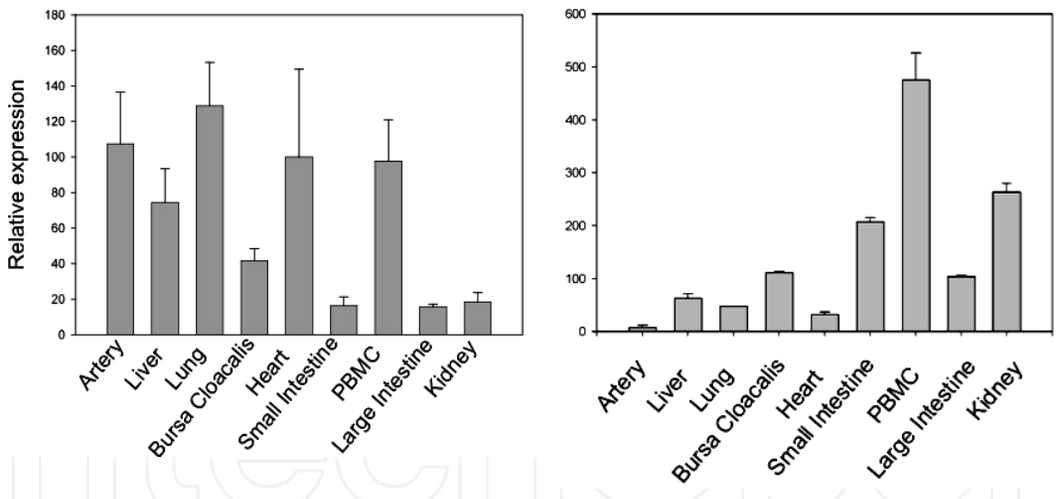

Figure 9. Relative expression of TLR1 and IκBα mRNA transcripts in vulture cells and tissues.

Real time RT-PCR was used to examine the relative amount of TLR1 (right) and IκB*α* (left) transcripts in vulture cells and tissues. The data were normalised using the beta-actin gene and calculated by the delta Ct method.

Moderate vulture TLR1 mRNA levels were observed in Bursa cloacalis and large intestine, whereas the lowest TLR1 mRNA levels were found in liver, heart and artery (Fig. 9). It has been reported that the patterns of TLR tissue expression are variable, even among closely related species (Zarember & Godowski 2002). Likewise, the intensity and the anatomic loca-

tion of the innate immune response may vary considerably among species (Rehli, 2002). Consistent with its role in pathogen recognition and host defense, the tissue and cell expression pattern of vulture TLR1, as revealed by real time RT-PCR, correlated with vulture ability to respond to various pathogenic challenges. The expression of vulture TLR1 was higher in cells such as circulating PBMC and intestinal epithelial cells that are immediately accessible to microorganisms upon infection.

The analysis of the relative expression of IκBα mRNA transcripts, using real-time RT-PCR, demonstrated that vulture IκBα mRNAs were higher in lung, artery, heart, and in PBMC cells (Fig. 9), which was consistent with its role in numerous physiological processes. Interestingly, the expression of vulture IκBα mRNA was observed in tissues at which the lowest expression of vulture Toll-like receptor was found. This is consistent with the role of IκBα as inhibitor of the TLR-signalling pathway.

6. Analysis of the evolutionary relationship of vulture TLR and IκBα

The dendrogram of sequences was calculated based on the distance matrix that was generated from the pairwise scores and the phylogenetic trees were constructed based on the multiple alignment of the sequences using the PHYLIP (Phylogeny Inference Package) available at the expasy.org web page. All ClustalW phylogenetic calculations were based around the neighbor-joining method of Saitou and Nei (Saitou & Nei, 1987).

For the analysis of the evolutionary relationship of vulture and other vertebrate TLR and IκBα, a phylogenetic tree was constructed with the TIR-domain sequences of human, macaque, bovine, pig, mouse, Japanese pufferfish and chicken TLR1. GenBank or swiss protein accessions numbers Q5WA51, Q706D2, Q6A0E8, Q59HI9, Q5H727 and Q5FWG5, respectively. The phylogenetic analysis of the TIR domain of vulture TLR1 revealed separate clustering of TLR1 from birds, fish, mouse and other mammals (Fig. 10B)

For the TLRs, it is assumed that the structure of the ectodomain has evolved more quickly than the structure of the TIR (Johnson, 2003). Similarly to other TLR receptors, the degree of homology of vulture TLR1 was higher in the transmembrane and cytoplasmic domains than in the extracellular domain. As expected, phylogenetic analysis of the TIR domains revealed separate clustering of TLR1 from birds, fish and mammals (Fig. 9B), suggesting independent evolution of the Toll family of proteins and of innate immunity (Beutler & Rehli, 2002; Roach et al., 2005).

The unrooted trees were constructed by neighbor-joining analysis of an alignment of the ankirin repeats of IκBα sequences from vulture and other species (A) or the alignment of the TIR domains of TLR1 from vulture and other species (B). The branch lengths are proportional to the number of amino acid differences. GenBank or swiss protein accessions numbers of chicken (*Gallus gallus*), human (*Homo sapiens*), mouse (*Mus musculus*), rat (*Rattus norvegicus*), African frog (*Xenopus laevis*), cattle (*Bos taurus*), zebrafish (*Danio rerio*), Mongolian gerbil (*Meriones unguiculatus*), Rainbow trout (*Oncorhynchus mykiss*) and pig (*Sus scrofa*) sequences

http://dx.doi.org/10.5772/54191

used for the phylogenetic tree were Q91974, P25963, Q08353, Q63746, Q1ET75, Q6DCW3, Q8WNW7, Q6K196, Q1ET75, Q8QFQ0 and Q9Z1E3, respectively.

For the analysis of the evolutionary relationship of vulture and other vertebrate IκBα, a phylogenetic tree was constructed with the sequences of chicken, human, mouse, rat, African frog, cattle, zebrafish, Mongolian gerbil, Rainbow trout and pig IκBα. The phylogenetic analysis of the ankyrin domain of vulture IκBα revealed separate clustering of IκBα from rodents, fish and other species and the sequence of vulture IκBα clustered together with that of chicken IκBα (Fig 10A). The IκB family includes IκBα, IκBβ, IκBγ, IκBε, IκBζ, Bcl-3, the precursors of NFκB1 (p105), and NF-κB2 (p100), and the Drosophila protein Cactus (Hayden et al., 2006; Karin & Ben-Neriah, 2000; Totzke et al., 2006; Gilmore, 2006). Why multiple IκB proteins now exist in vertebrates has been a subject of great interest, and much effort has been expended on establishing the roles of individual members of this protein family in the regulation of NF-κB. The recent identification of a novel member of IκB family (IκBζ) indicates that there might exist species-specific differences in the regulation of NF-κB (Totzke et al., 2006).

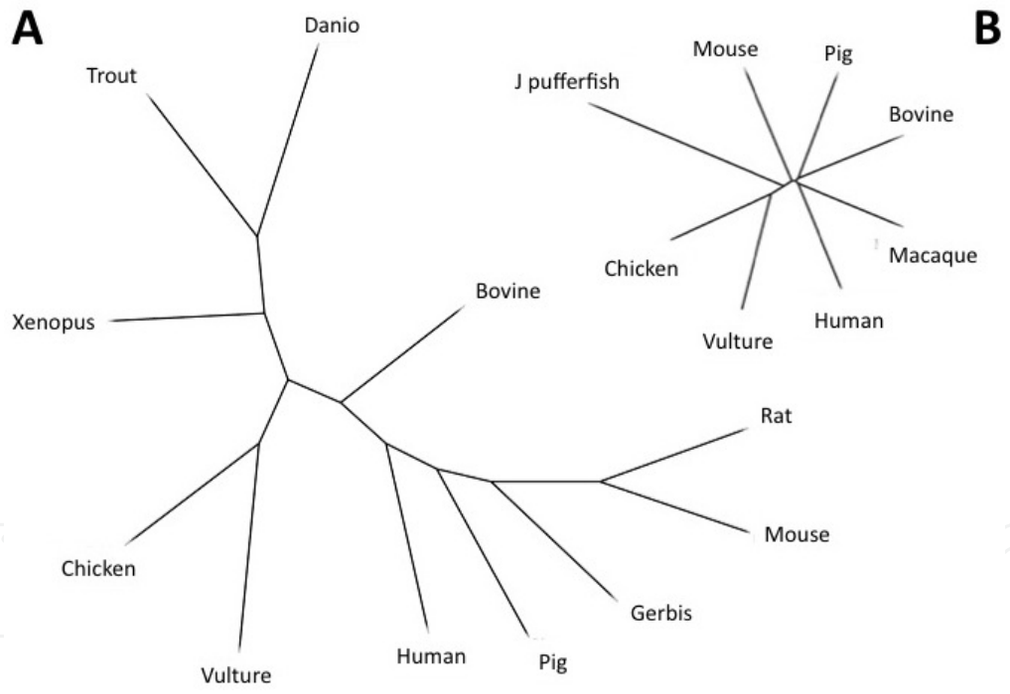

Figure 10. Phylogenetic trees illustrating the relationship between TLR and IκBα sequences from vulture and other species.

Evolutionarily, the IκB protein family is quite old, as members have been found in insects, birds and mammals (Ghosh & Kopp, 1998). However, the finding that individual ankyrin repeats within each IκB molecule are more similar to corresponding ankyrin repeats in other IκB family members, rather than to other ankyrin repeats within the same IκB, suggests that all IκB family members evolved from an ancestral IκB molecule (Huguet, et al., 1997).

Consistent with the hypothesis that all these factors evolved from a common ancestral RHD-ankyrin structure within a unique superfamily, explaining the specificities of interaction between the different Rel/NF-kappa B dimers and the various I kappa B inhibitors (Huguet, et al., 1997).

Recently, the presence of two IkappaB-like genes in Nematostella encoded by loci distinct from nf-kb suggested that a gene fusion event created the nfkb genes in insects and vertebrates (Sullivan et al., 2007). This is consistent with the hypothesis that interactions between transcription factors of the Rel members and members of the IκB gene family evolved to regulate genes mainly involved in immune inflammatory responses (Bonizzi & Karin, 2004).

NF-kappaB represents an ancient, generalized signaling system that has been co-opted for immune system roles independently in vertebrate and insect lineages (Friedman & Hughes, 2002). Therefore, while these proteins share a basic three-dimensional structure as predicted by their shared ankyrin repeat pattern and sequence, a possible evolutionary scenario based on this phylogenetic tree could be that subtle differences in the amino acid substitutions in the ankyrin repeats and flanking sequences occurred throughout evolution, which contributed to their specificity of interaction with various members of the Rel family.

7. Summary

The ORFs reported herein identified and characterized the vulture orthologues to TLR1 (CD281) and to IκBα, the first NF-κB pathway element from the griffon vulture *G. fulvus*. In addition, we have also identified sequences that may be involved in the protection of vultures against toxins. These results have implications for the understanding of the evolution of pathogen-host interactions. Particularly, these studies help to highlight a potentially important regulatory pathway for the study of the related functions in vulture immune system (Perez de la Lastra & de la Fuente, 2007; 2008). Despite the overall structure of vulture TLR1 and expression pattern was similar to that of chicken, pig, cattle, human and mouse TLR, vulture TLR1 had differences in the length of the ectodomain, number and position of LRRs and N-glycosylation sites that makes vulture TLR1 structurally unique with possible functional implications.

Strong selective pressure for recognition of and response to pathogen-associated molecular patterns (PAMPs) has probably maintained a largely unchanged TLR signalling pathways in all vertebrates. The IκBα gene reported here expands our understanding of the immune regulatory pathways present in carrion birds that are in permanent contact with pathogens. Current investigations should focus on the cloning and characterization of other members of NF-κB signalling cascade and genes controlled by this signalling pathway. At this point it is difficult to understand the implications of the structural differences between vulture TLR1, chicken TLR1 and TLR1 in different mammalian species. A greater understanding of the functional capacity of non-mammalian TLRs and, particularly in carrion birds that are in permanent contact with pathogens, has implications for the understanding of the evolutionary pressures that defined the TLR repertoires in present day animals. The discovery of mol-

http://dx.doi.org/10.5772/54191

ecules that neutralize toxins found in the genetic and phenotypic background of an organism (like vulture) is extremely adequate for bio compatible drugs and antidote development.

8. Biotechnological applications of molecules involved in the recognition of pathogens

Our growing understanding of host-pathogen interactions and mechanisms of protective immunity have allowed for an increasingly rational approach to the design of immune based therapeutics. One posible biomedical application of the discovery of efficient pathogen receptors could be the generation of "immunoadhesins" (Perez de la Lastra et al., 2009). Because of the versatility of immunoadhesins, immunoadhesin-based therapies could, in theory, be developed against any existing pathogen. Some advantages of immunoadhesin-based therapies include versatility, low toxicity, pathogen specificity, enhancement of immune function, and favorable pharmacokinetics; the disadvantages include high cost, limited usefulness against mixed infections and the need for early and precise microbiologic diagnosis.

The patent by Visintin *et al*. (cited in Perez de la Lastra et al., 2009) discloses anti-pathogen immunoadhesins (APIs), a subset of which is "tollbodies", which have a pathogen recognition module derived from the binding domain of a toll-like receptor (TLR). A schematic illustration of an exemplary API is shown in Fig. 11.

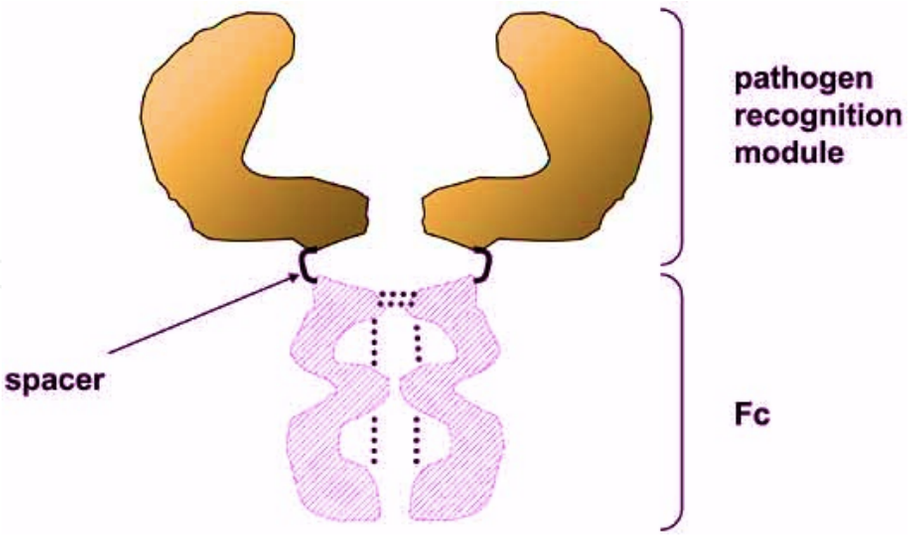

Figure 11. Schematic structure of an anti-pathogen immunoadhesin (API). Gray undashed area, pathogen recognition module; dashed, Fc portion. Disulfide bridges are represented by dashed line, which include intrachain bridges (that stabilize the Ig domains) and the interchain bridges (that covalently link two immunoadhesin molecules).

APIs can be used as therapeutics, e.g., for treating pathogen-associated disorders, e.g., infections and inflammatory conditions (e.g. inflammatory conditions associated with a patho-

gen- associated infection) and other disorders in which it is desirable to inhibit signaling pathways associated with the pathogen recognition protein from which the extracellular domain of the API is derived. These APIs are particularly useful therapeutics because pathogens generally cannot mutate the PAMPs (e.g., LPS) that are recognized by the pathogen recognition proteins. Thus, APIs can be used as antipathogenic agents to whom the targeted pathogen cannot develop resistance. The APIs can thus be used both *in vivo* and *in vitro/ex vivo*, e.g. to remove pathogens from blood or a water supply, or other liquids to be consumed, e.g., beverages, or even in the air, e.g. to combat a weapon of biological warfare. It is envisaged that these immunotechnological advances will increase the available antiinfective armamentarium and that immunoadhesin-therapy is poised to play an important part in modern anti-infective drugs.

Acknowledgements

This work was supported by the Junta de Comunidades de Castilla-La Mancha (JCCM), project PII1I09-0243-4350.

Author details

Lourdes Mateos-Hernández[1], Elena Crespo[1], José de la Fuente[1,2] and José M. Pérez de la Lastra[1]

1 Instituto de Investigación en Recursos Cinegéticos (UCLM-CSIC-JCCLM), Ronda Toledo s/n, Ciudad Real, Spain

2 Department of Veterinary Pathobiology, Center for Veterinary Health Sciences, Oklahoma State University, Stillwater, OK, USA

References

[1] Aoki, T., et al., The ankyrin repeats but not the PEST-like sequences are required for signal-dependent degradation of IkappaBalpha. Oncogene, 1996. 12(5): p. 1159-64.

[2] Apanius, V., S.A. Temple, and M. Bale, Serum proteins of wild turkey vultures (Cathartes aura). Comp Biochem Physiol B, 1983. 76(4): p. 907-13.

[3] Beutler, B. and M. Rehli, Evolution of the TIR, tolls and TLRs: functional inferences from computational biology. Curr Top Microbiol Immunol, 2002. 270: p. 1-21.

[4] Bonizzi, G. and M. Karin, The two NF-kappaB activation pathways and their role in innate and adaptive immunity. Trends Immunol, 2004. 25(6): p. 280-8.

[5] Bourne, H.R., D.A. Sanders and F. McCornick, The GTPase superfamily: conserved structure and molecular mechanism. Nature, 1991. 349: p. 117-126.

[6] Brown, K., et al., The signal response of IkappaB alpha is regulated by transferable N- and C-terminal domains. Mol Cell Biol, 1997. 17(6): p. 3021-7.

[7] Desterro, J.M., M.S. Rodriguez, and R.T. Hay, SUMO-1 modification of IkappaBalpha inhibits NF-kappaB activation. Mol Cell, 1998. 2(2): p. 233-9.

[8] Eidels, L., R.L. Proia and D.A. Hart, Membrane receptors for bacterial toxins. Microbiol Rev, 1983. 47: p. 596-620.

[9] Friedman, R. and A.L. Hughes, Molecular evolution of the NF-kappaB signaling system. Immunogenetics, 2002. 53(10-11): p. 964-74.

[10] Ghosh, S., M.J. May, and E.B. Kopp, NF-kappa B and Rel proteins: evolutionarily conserved mediators of immune responses. Annu Rev Immunol, 1998. 16: p. 225-60.

[11] Gilmore, T.D., Introduction to NF-kappaB: players, pathways, perspectives. Oncogene, 2006. 25(51): p. 6680-4.

[12] Hayden, M.S., A.P. West, and S. Ghosh, NF-kappaB and the immune response. Oncogene, 2006. 25(51): p. 6758-80.

[13] Hopkins, P.A. and S. Sriskandan, Mammalian Toll-like receptors: to immunity and beyond. Clin Exp Immunol, 2005. 140(3): p. 395-407.

[14] Houston, D.C. and J.E. Cooper, The digestive tract of the whiteback griffon vulture and its role in disease transmission among wild ungulates. J Wildl Dis, 1975. 11(3): p. 306-13.

[15] Huguet, C., P. Crepieux, and V. Laudet, Rel/NF-kappa B transcription factors and I kappa B inhibitors: evolution from a unique common ancestor. Oncogene, 1997. 15(24): p. 2965-74.

[16] Jaffray, E., K.M. Wood, and R.T. Hay, Domain organization of I kappa B alpha and sites of interaction with NF-kappa B p65. Mol Cell Biol, 1995. 15(4): p. 2166-72.

[17] Johnson, G.B., et al., Evolutionary clues to the functions of the Toll-like family as surveillance receptors. Trends Immunol, 2003. 24(1): p. 19-24.

[18] Karin, M. and Y. Ben-Neriah, Phosphorylation meets ubiquitination: the control of NF-[kappa]B activity. Annu Rev Immunol, 2000. 18: p. 621-63.

[19] Krishnan, V.A., et al., Structure and regulation of the gene encoding avian inhibitor of nuclear factor kappa B-alpha. Gene, 1995. 166(2): p. 261-6.

[20] Luque, I. and C. Gelinas, Distinct domains of IkappaBalpha regulate c-Rel in the cytoplasm and in the nucleus. Mol Cell Biol, 1998. 18(3): p. 1213-24.

[21] Luque, I., et al., N-terminal determinants of I kappa B alpha necessary for the cytoplasmic regulation of c-Rel. Oncogene, 2000. 19(9): p. 1239-44.

[22] Mabb, A.M. and S. Miyamoto, SUMO and NF-kappaB ties. Cell Mol Life Sci, 2007. 64(15): p. 1979-96.

[23] Ohishi, I., et al., Antibodies to Clostridium botulinum toxins in free-living birds and mammals. J Wildl Dis, 1979. 15(1): p. 3-9.

[24] Perez de la Lastra, J.M. and J. de la Fuente, Molecular cloning and characterisation of the griffon vulture (Gyps fulvus) toll-like receptor 1. Dev Comp Immunol, 2007. 31(5): p. 511-9.

[25] Perez de la Lastra, J.M. and J. de la Fuente, Molecular cloning and characterisation of a homologue of the alpha inhibitor of NF-kB in the griffon vulture (Gyps fulvus). Vet Immunol Immunopathol, 2008. 122: p. 318-25

[26] Perez de la Lastra, J.M., L. Kremer and J. De la Fuente, Recent advances in the development of immunoadhesins for immune therapy and as anti-infective agents. Recent Patents on Anti-Infective Drug Discovery, 2009, 4: p. 183-189.

[27] Pons, J., et al., Structural studies on 24P-IkappaBalpha peptide derived from a human IkappaB-alpha protein related to the inhibition of the activity of the transcription factor NF-kappaB. Biochemistry, 2007. 46(11): p. 2958-72.

[28] Roach, J.C., et al., The evolution of vertebrate Toll-like receptors. Proc Natl Acad Sci U S A, 2005. 102(27): p. 9577-82.

[29] Saitou, N. and M. Nei, The neighbor-joining method: a new method for reconstructing phylogenetic trees. Mol Biol Evol, 1987. 4(4): p. 406-25.

[30] Shumway, S.D., M. Maki, and S. Miyamoto, The PEST domain of IkappaBalpha is necessary and sufficient for in vitro degradation by mu-calpain. J Biol Chem, 1999. 274(43): p. 30874-81.

[31] Sullivan, J.C., et al., Rel homology domain-containing transcription factors in the cnidarian Nematostella vectensis. Dev Genes Evol, 2007. 217(1): p. 63-72.

[32] Takeda, K. and S. Akira, Toll-like receptors in innate immunity. Int Immunol, 2005. 17(1): p. 1-14.

[33] Takeda, K., Evolution and integration of innate immune recognition systems: the Toll-like receptors. J Endotoxin Res, 2005. 11(1): p. 51-5.

[34] Totzke, G., et al., A novel member of the IkappaB family, human IkappaB-zeta, inhibits transactivation of p65 and its DNA binding. J Biol Chem, 2006. 281(18): p. 12645-54.

[35] Weber, A.N., M.A. Morse, and N.J. Gay, Four N-linked glycosylation sites in human toll-like receptor 2 cooperate to direct efficient biosynthesis and secretion. J Biol Chem, 2004. 279(33): p. 34589-94.

IntechOpen

IntechOpen